Interpreting the Dynamic Interaction between a Very Small Rising Bubble and a Hydrophilic Titania Surface

Rogerio Manica,[†] Luke Parkinson,[‡] John Ralston,[‡] and Derek Y. C. Chan*[,§,∥]

Institute of High Performance Computing, 1 Fusionopolis Way, Number 16-16 Connexis, 138632 Singapore, Ian Wark Research Institute, University of South Australia, Mawson Lakes SA 5095, Australia, Particulate Fluids Processing Centre, Department of Mathematics and Statistics, The University of Melbourne, Parkville VIC 3010 Australia, and Department of Mathematics, National University of Singapore, 117543 Singapore

Received: November 23, 2009; Revised Manuscript Received: December 10, 2009

We interpret recent measurements of time-varying interference fringe intensities observed between rising bubbles (diameter 15−120 μm) and a horizontal hydrophilic titania plate to determine the rate of approach of such bubbles to the surface. The bubbles remain spherical because of high Laplace pressures and small buoyancy forces so the approach velocity remains in the Stokes flow regime. The rate of approach of the bubble to the titania plate is controlled by buoyancy force and surface forces such as van der Waals and electric double layer interactions together with a hydrodynamic force arising from the drainage of the thin water film between the bubble and the titania surface. The dynamics are found to be consistent with the no-slip hydrodynamic boundary condition at the surface of the bubble and at the titania plate. However, far from the titania plate the terminal velocities of the rising bubbles suggests that the bubble surfaces are fully mobile with zero tangential stress.

Introduction

Parkinson and Ralston[1] reported detailed measurements of the dynamics of the approach of single bubbles (15−120 μm in diameter) rising under buoyancy force in an aqueous electrolyte toward a smooth horizontal titania plate. The experimental data were in the form of high-speed recordings (1000 frames per second) of time varying interference intensity fringes between the bubble surface and the titania surface as the bubble approached. From the intensity pattern of these fringes, it is possible to infer the shape of the bubbles and the time variation of the separation between the bubble and titania plate with a resolution to better than 10 nm. A related technique has been used recently to quantify the deformations and the separation between a mercury drop and a surface[2,3] and between approaching drops in various liquids.[4,5] The electrical double layer interaction between the titania plate and the bubble can be controlled by changing the electrolyte concentration. With the solution pH set to above and below the titania isoelectric point, the sign of the titania surface charge can be reversed. Our goal is to develop a theoretical model to interpret these measurements and to quantify the parameters that determine dynamic bubble−surface interaction in this system.

Under identical solution conditions, results of terminal rise velocity measurements are consistent with the bubble surface being a fully mobile interface that cannot support any shear stress and, as such, the terminal velocity obeys the Hadamard−Rybczynski formula.[6] However, it has been observed that even small traces of surfactant in the system are enough to cause the bubble surface to behave as an immobile (no-slip) interface.[6−9] One objective of our modeling is to investigate the boundary condition that holds at the liquid−vapor interface when the bubble is close to the surface. Comparisons between theory and experiments are performed for a matrix of experimental conditions at pH 6.3 that gives rise to repulsive double layer interactions between the bubble and the surface with two different salts: KCl and $N(CH_3)_4Br$ for five different concentrations ranging from no salt to 10^{-1} M. For each case, the results corresponding to at least three bubbles of different diameters are analyzed.

Experimental Method and Analysis

In the experimental apparatus, a bubble of radius R is allowed to rise under gravity before striking a transparent titania (TiO_2) surface. Readers are referred to Parkinson and Ralston[1] for details of the experiments. The goal is to deduce time variations of the distance of closest approach, $h(t)$ between the bubble and the surface. The interference fringes between the titania/electrolyte and the air/electrolyte interface are recorded using a high-speed camera at 1000 fps. Time variations of the intensity $I(t)$ at the center of the fringe pattern can be converted to the distance of closest approach $h(t)$ between the bubble and the titania surface through the following relation[10]

$$\frac{I(t) - I_{min}}{I_{max} - I_{min}} = \sin^2\left(\frac{2\pi n h(t)}{\lambda_0}\right) \quad (1)$$

where I_{max} and I_{min} are the maximum and minimum intensity, respectively, λ_0 (550 nm) is the wavelength of light in air, and n (1.333) is the refractive index of water.

The radii of the bubbles were kept to below 60 μm to ensure that the Reynolds number ($Re = 2\rho R V_{St}/\mu$) does not exceed 1, where ρ is the density, μ the viscosity of water, and V_{St} the terminal rise velocity calculated from the Stokes formula: $V_{St} = (2/9)(\rho R^2 g/\mu)$ where g is the acceleration due to gravity.

* To whom correspondence should be addressed. Phone: + 61-3-8344-5556. Fax: + 61-3-8344-4599. E-mail: D.Chan@unimelb.edu.au.
[†] Institute of High Performance Computing.
[‡] University of South Australia.
[§] The University of Melbourne.
[∥] National University of Singapore.

10.1021/jp911104b
Published on Web 12/30/2009

Therefore, Stokes flow is appropriate for this system and we can introduce surface forces to the known solutions of a sphere approaching a horizontal surface to model the rise of the bubble toward the titania plate under the influence of hydrodynamic and colloidal surface forces. Under Stokes flow, the equation that determined the distance of closest approach, $h(t)$, between the bubble and the surface can be written in the form

$$6\pi\mu R\Lambda(h)\frac{dh}{dt} = -\frac{4}{3}\pi R^3\rho g + 2\pi R[E_{vdW}(h) + E_{EDL}(h)] \quad (2)$$

The first term on the RHS is the buoyancy force, E_{vdW} and E_{EDL} are, respectively, the van der Waals and electrical double layer interaction energy per unit area between the bubble and the titania surface and they are related to the corresponding force via the Deryaguin approximation. These forces are balanced by the hydrodynamic drag force F_d on the LHS where the form of the function $\Lambda(h)$ depends on the nature of the hydrodynamic boundary conditions on the surfaces.

At the solid titania plate, the no-slip boundary applies and the fluid velocity vanishes there. At the bubble surface, the usual assumption is that the liquid−vapor interface cannot sustain any shear stress and is commonly referred to as a fully mobile interface with the corresponding expression for $\Lambda(h)$ given by Bart.[11] If on the other hand, the no-slip boundary condition holds at the bubble surfaces, then the result for $\Lambda(h)$ is given by Brenner.[12] Both results are expressed as infinite series that converges rather slowly when the bubble is close to the surface ($h/R \rightarrow 0$). The exact series expressions for $\Lambda(h)$ are given in the Appendix where we also offer simple and accurate analytic approximations to them. These analytic approximations have the correct asymptotic forms in the limit of small and large (h/R):

$$\Lambda(h) \rightarrow \begin{cases} 1, & (h/R) \rightarrow \infty \\ (R/h), & (h/R) \rightarrow 0 \end{cases} \quad \text{no-slip bubble} \quad (3a)$$

$$\Lambda(h) \rightarrow \begin{cases} (2/3), & (h/R) \rightarrow \infty \\ (R/4h), & (h/R) \rightarrow 0 \end{cases} \quad \text{fully-mobile bubble} \quad (3b)$$

In both cases, $\Lambda(h)$ diverges as $1/h$ as the separation approaches zero, so dh/dt will approach zero and the bubble will attain a final equilibrium separation h_{eq} determined solely by surface forces. If there are mobile surface active species at the bubble surface, the form of $\Lambda(h)$ will lie between the results given by Brenner and Bart but the exact form depends on the mobility of the mobile surface species.

With a no-slip bubble, we have the Taylor limit $F_d = -6\pi\mu(R^2/h)\,(dh/dt)$ since $\Lambda(h) \rightarrow (R/h)$ as $h/R \rightarrow 0$ and eq 2 becomes

$$\frac{6\pi\mu R^2}{h}\frac{dh}{dt} = -\frac{4}{3}\pi R^3\rho g + 2\pi R[E_{vdW}(h) + E_{EDL}(h)] \quad (4)$$

In the case of high salt concentration in which electrical double-layer interaction (E_{EDL}) can be neglected, and with the repulsive van der Waals interaction (neglecting electromagnetic retardation effects) having the form $E_{vdW} = -A/(12\pi h^2)$, with Hamaker constant $A = -4 \times 10^{-20}$ J < 0 for the TiO_2|water|air system,

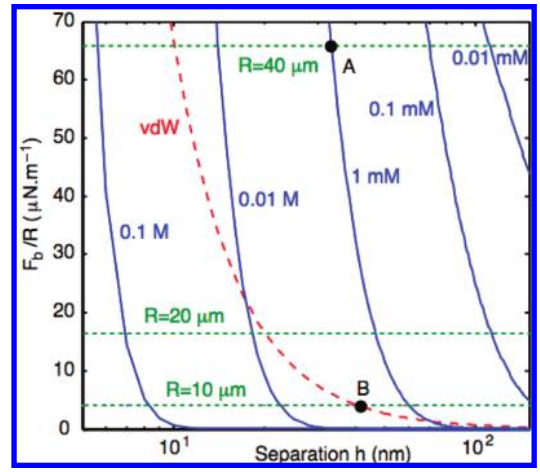

Figure 1. Forces on a bubble: van der Waals interaction (red - - -) with Hamaker constant $A = -4 \times 10^{-20}$ J and electrical double layer interaction (blue —) for 10^{-5} to 10^{-1} M 1:1 electrolyte and surface potentials $\Psi = -45$ mV (titania)1 and −60 mV (bubble).[14] The buoyancy force, $F_b = (4\pi/3)\rho g R^3$ (green - - -), for three different bubble radii is also plotted.

eq 4 can be easily integrated to give variations of the bubble-titania separation as a function of time:

$$h(t) = \sqrt{\eta^2 + (h_0^2 - \eta^2)e^{-2t/\tau}} \quad (5)$$

where h_0 is the initial separation, $\eta^2 = |A|/(8\pi\rho g R^2)$ and $\tau = 9\,\mu/(2\rho g R)$. A similar result can be obtained for the fully mobile bubble in the limit $h/R \rightarrow 0$.

The electrical double layer interaction free energy per unit area can be calculated from the superposition approach for $\kappa h > 2$ as[13]

$$E_{EDL} = \frac{64 n_o kT}{\kappa}\tanh\left(\frac{y_1}{4}\right)\tanh\left(\frac{y_2}{4}\right)e^{-\kappa h} \quad (6)$$

where n_o is the number concentration of 1:1 electrolyte, k the Boltzmann constant, T the temperature, $1/\kappa$ the Debye length, and $\Psi_i = kTy_i/e$ ($i = 1,2$), is the surface potential on the bubble or on the titania plate. As we shall see, the equilibrium film thicknesses, h_{eq} are always larger than the Debye length ($\kappa h_{eq} > 1$) which justifies the use of eq 6. Furthermore in the superposition limit, we need not be concerned with whether the surfaces interact under constant surface charge or surface potential.

Results and Discussions

A comparison of the relative magnitudes of different forces acting on the bubble is given in Figure 1 at pH 6.3 where the electrical double layer interaction is repulsive. For low salt concentrations, the electrical double layer interaction dominates, so for instance, the equilibrium separation between a bubble with a radius of 40 μm and the surface at 1 mM salt is given by point A in Figure 1. At high salt concentrations, the van der Waals repulsion dominates and the equilibrium position, for example, of a bubble with a radius of 10 μm radius at 0.1 M salt is indicated by point B in Figure 1. Intermediate concentrations generally require the consideration of both the electrical double layer and van der Waals forces as illustrated in the example of a bubble with a radius of 20 μm radius at 0.01 M in Figure 1.

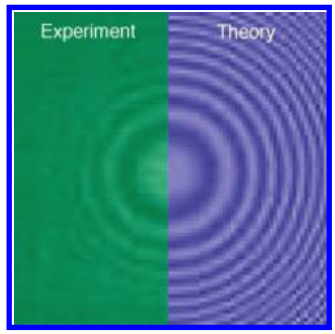

Figure 2. Snapshot of the experimental intensity fringes (LHS) with resolution of 0.34 mm per pixel compared to theoretically generated fringes (RHS) for a bubble at equilibrium against the titania plate in 0.1 M $N(CH_3)_4Br$ electrolyte. The bubble radius is 50 μm, the surface potentials are −45 mV (titania)[1] and −60 mV (bubble),[14] and the equilibrium separation is $h_{eq} = 20$ nm.

We first consider the fringe intensity of a bubble resting at its equilibrium position after it has risen to the titania plate. In Figure 2 we compare the form of experimental fringe intensity (left side) with the theoretical intensity (right side) calculated using eqs 1 and 2 for a bubble resting at the plate at an equilibrium separation h_{eq} determined by a balance of buoyancy and electrical double forces ($h_{eq} = 20$ nm). The bubble surface is assumed to be spherical, with $h(r) = h_{eq} + r^2/(2R)$, where $R = 50$ μm is the measured bubble radius. We see excellent agreement in the fringe intensity pattern using measured system parameters as input to the theory. As this comparison is for one of the largest bubbles in the experimental range, we are confident that the smaller bubbles are also spherical and not deformed as a result of interactions.

From eq 1, we see that the rate of approach of the bubble toward the titania plate is related to the time variation of the intensity at the center of the fringe pattern. We therefore model this variation using two extreme models for the hydrodynamic boundary condition at the bubble surface: an immobile interface that obeys the "no-slip" boundary condition and the bubble behaves hydrodynamically like a solid particle or a tangentially mobile interface that will not support any shear stress. The results in parts a and b of Figure 3 for a bubble at 0.1 mM KCl approaching the titania surface demonstrates unambiguously that time variations of the central fringe intensity $I(t)$ (Figure 3a) or equivalently time variations of the separation $h(t)$ between the bubble and the titania plate (Figure 3b) coincide with the theoretical predictions for an immobile ("no-slip") condition at the air/water interface of the bubble surface. The key observation is the excellent agreement between experiments and the predictions of the "no-slip" boundary condition for the periodicity of the intensity oscillations that directly reflects the rate of film thinning. The slightly lower amplitudes in the intensities at early times are due to attenuation and scattering by the thicker water film. The results in parts c and d of Figure 3 demonstrate that modeling the primary intensity data, and in particular the periodicity of the intensity variation, provides a more sensitive test between experiment and theory than modeling the monotonically decreasing separation $h(t)$. For instance, the disagreement between the theoretical and experimental intensity at large times is quite marked while the corresponding difference in the equilibrium separation h_{eq} appears rather small. Predictions using the fully mobile instead of the "no-slip" boundary condition at the bubble surface for parts c and d of Figure 3 give similar results as in parts a and b of Figure 3 in that the period of the oscillations in the intensity is too short and thus the separation $h(t)$ decreases too rapidly.

Comparisons between theory and experiment for most bubbles studied showed that the rate of approach of the bubble toward the titania plate at small times when hydrodynamic effects dominate is consistent with the immobile "no-slip" hydrodynamic boundary conditions using values of bubble radii that are within the experimental uncertainty of 2 μm of the measured bubble sizes. However, measurements of bubble terminal velocity prior to any interaction with the titania surface show results that are accurately predicted by the Hadamard−Rybczynski formula, which is derived under the assumption of a tangentially

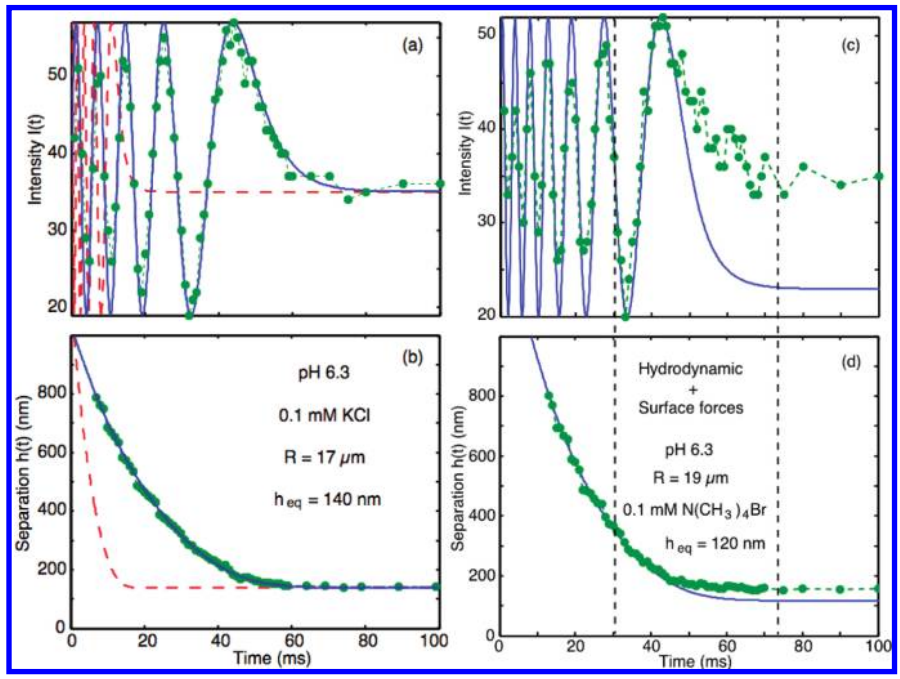

Figure 3. Comparison between theory and experiment using the immobile ("no slip") (blue —) and fully mobile (red - - -) boundary conditions at the bubble surface for (a) the fringe central intensity and (b) the corresponding separation at 0.1 mM KCl. Similar comparison for 0.1 mM $N(CH_3)_4Br$ are in parts c and d. The surface potentials are taken to be −45 mV (titania)[1] and −60 mV (bubble).[14]

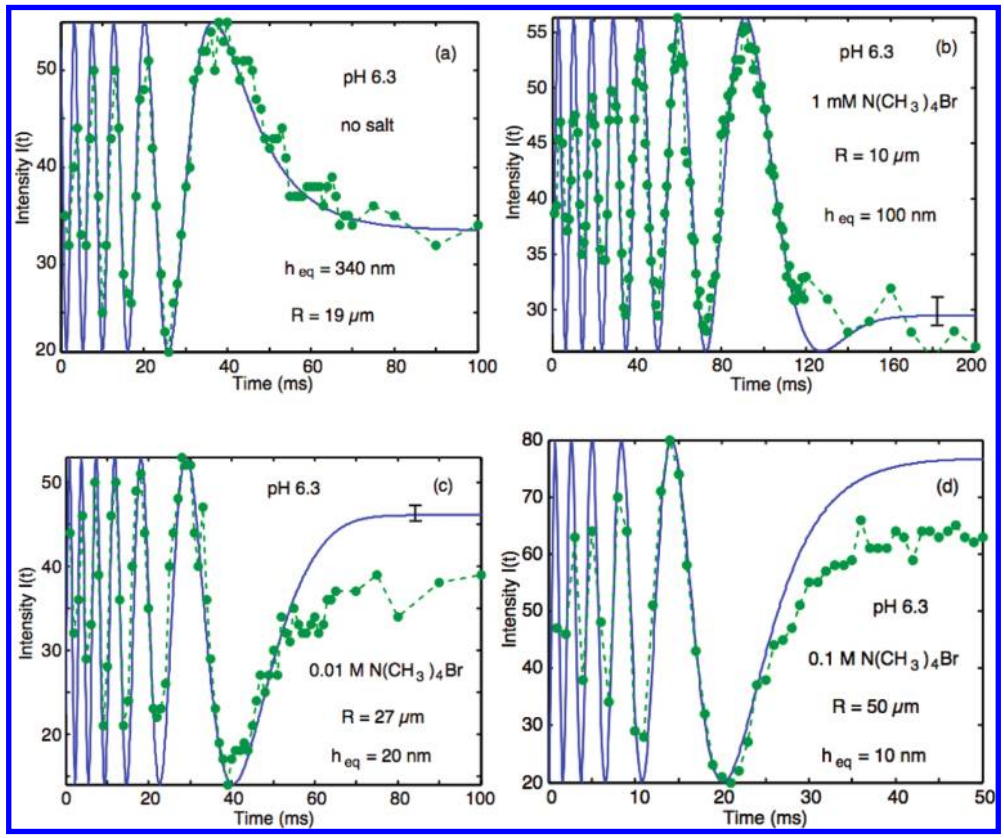

Figure 4. Comparison between theory and experiment for different salt concentrations ranging from no salt added to 0.1 M. Details of each experiment are given in the figure. The surface potential of the titania and bubble surfaces are taken to be −45 and −60 mV, respectively.

mobile bubble surface. Possible reasons for the observed change in the boundary condition have been proposed.[1]

The results in Figure 3c,d also illustrate the different separation regimes of the bubble−plate interaction. In this particular example, only hydrodynamic effects are important for times smaller than 30 ms when the separation is sufficiently large and that the influence of surface forces may be neglected. For time larger than 70 ms, only surface forces are important because the bubble is almost stationary and so there are no hydrodynamic effects. At intermediate times, between 30 and 70 ms, both hydrodynamic and surface force effects combine to influence the motion of the bubble.

Over 60 experimental data sets have been analyzed with satisfactory agreement for different salts, ionic strengths, and bubble sizes. The cases of low electrolyte concentrations where double layer interactions are dominant and equilibrium separations are large gave better agreement overall compared to the cases of small equilibrium separations. We selected one representative case of each electrolyte concentration and present the results in Figure 4. As the electrolyte concentration is increased, the equilibrium thickness decreases, which is expected since the electrical double layer becomes shorter ranged with increasing electrolyte concentration, see parts a−c of Figure 4. In these cases, the intensities at large times are determined mainly by the electrolyte concentration. The rather small effects at large times due to variations of the bubble surface potentials between −30 and −100 mV are indicated by the error bars. At very low salt concentrations (Figure 4a), the surface potential and the unknown salt concentration are treated as fitting parameters: −60 mV and 3.5×10^{-6} M. However, the same parameters will reproduce measured intensities from the same batch of bubbles. At 0.1 M salt (Figure 4d), the equilibrium thickness is determined only by repulsive van der Waals

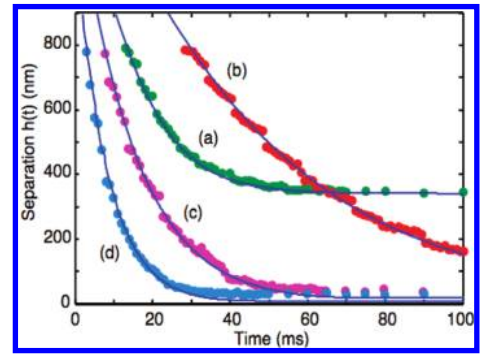

Figure 5. Bubble−titania plate separation $h(t)$ corresponding to the intensity functions of Figure 4. The labels a−d of the theoretical curves and experimental data points refer to the plots in Figure 4.

interactions between the bubble and the titania surface since all electrostatic interactions are screened out. This is a practical manifestation of repulsive Lifshitz−van der Waals interactions that has attracted recent interest in the context of quantum levitation.[15]

The time evolution of the bubble position $h(t)$ that corresponds to the results in Figure 4 are presented in Figure 5 with curves a−d matching the respective plots in Figure 4. These results demonstrate that the rate of approach of the bubbles to the titania surface increases with bubble radius due to the larger buoyancy forces and illustrate the importance of electrolyte concentration on the equilibrium position of the bubbles.

Conclusions

The analysis presented in this paper has succeeded in providing an accurate description of small bubbles rising under gravity under Stokes flow. It combines in one model the three

different phases of interaction that arise (i) from hydrodynamic drag when the bubble is far from the titania plate, (ii) from both hydrodynamic interactions, given by the Brenner theory and surface forces represented by electrical double layer and van der Waals interactions that retard the bubble at intermediate separations, and finally (iii) near equilibrium where only surface forces are relevant in determining the equilibrium separation. The theory compares well against the experimental data for all times and is flexible enough to be adapted to similar systems with different surface forces or boundary conditions.

The primary experimental results are the measured intensity data of the interference fringes, and our theoretical approach in analyzing the experimental data is therefore to model the evolution of the fringe intensities directly. This proved to be a sensitive test between experiment and theory. Furthermore, measuring the periodic time variation in a reflected light interference pattern is a sensitive way to deduce the separation between the bubble and the surfaces.

The immobile boundary condition for the air−water interface provided the best agreement between theory and experiments even though the initial bubble rise velocity appears consistent with a fully mobile interface. While extreme care has been taken to ensure cleanliness in our experimental system as demonstrated by bubble rise velocities being consistent with a fully mobile bubble surface, we cannot completely rule out the possibility of contamination in the solution in the close proximity of the titania surface. Trace amounts of surface-active contaminants are sufficient to arrest hydrodynamic mobility at the bubble surface and cause the "no-slip" to hold at the bubble surface.[8,9] We recognize that ion concentration gradients during flow may also induce similar effects.[1]

Acknowledgment. Financial support from the Australian Research Council Linkage Grants Scheme, AMIRA International, and the State Governments of Victoria and South Australia is gratefully acknowledged. D.Y.C.C. is an Adjunct Professor at the National University of Singapore.

Appendix

Under Stokes flow, the drag force of a spherical bubble of radius R with zero viscosity moving perpendicular to a no-slip flat surface at velocity V in a fluid of shear viscosity μ can be written as

$$F_d = 6\pi\mu RV\Lambda(h) \tag{A1}$$

where $0 < h < \infty$ is the distance of closest approach between the sphere and the surface.

If the shear stress vanishes at the bubble surface, the fully mobile boundary condition, the function $\Lambda(h)$, is given by[11]

$$\Lambda(h) = \sum_{n=0}^{\infty} K_n \times \left\{\frac{2e^{-(2n+1)\alpha} + 2\cosh(2\alpha) + (2n+1)\sinh(2\alpha)}{2\sinh[(2n+1)\alpha] - (2n+1)\sinh(2\alpha)}\right\} \tag{A2a}$$

$$\cong \frac{1 + 8.11x + 7.44x^2}{(8/3)x + 7.44x^2}, \quad x = h/R \tag{A2b}$$

where $K_n = 4/3\ \sinh(\alpha)\ (n(n+1)/(2n-1)(2n+3))$ and $2\sinh^2(\alpha/2) = (h/R)$. The approximate formula (eq A2b) agrees with the infinite series (eq A2a) to within ±1.5% for all $0 < (h/R) < \infty$ and has the exact limiting behavior given by eq 3a.

If the no-slip boundary condition holds at the bubble surface, the function $\Lambda(h)$ is given by[12]

$$\Lambda(h) = \sum_{n=0}^{\infty} K_n \times \left\{\frac{2\sinh[(2n+1)\alpha] + (2n+1)\sinh(2\alpha)}{4\sinh^2[(2n+1)(\alpha/2)] - (2n+1)^2\sinh^2(2\alpha)} - 1\right\} \tag{A3a}$$

$$\cong \frac{1 + 2.34x + (17/8)x^2 + x^3}{x + x^2 + x^3} \tag{A3b}$$

The approximate formula (eq A3b) agrees with the infinite series (eq A3a) to within ±1.3% for all $0 < (h/R) < \infty$ and has the exact limiting behavior given by eq 3b. The Padè approximants in eqs A2b and A3b given here should be sufficiently accurate for most applications.

References and Notes

(1) Parkinson, L.; Ralston, J. *J. Phys. Chem. C* submitted.
(2) Connor, J. N.; Horn, R. G. *Faraday Discuss.* **2003**, *123*, 193.
(3) Manica, R.; Connor, J. N.; Carnie, S. L.; Horn, R. G.; Chan, D. Y. C. *Langmuir* **2007**, *23*, 626.
(4) Klaseboer, E.; Chevaillier, J. Ph.; Gourdon, C.; Masbernat, O. *J. Colloid Interface Sci.* **2000**, *229*, 274.
(5) Manica, R.; Klaseboer, E.; Chan, D. Y. C. *Soft Matter* **2008**, *4*, 1613.
(6) Parkinson, L.; Sedev, R.; Fornasiero, D.; Ralston, J. *J. Colloid Interface Sci.* **2008**, *322*, 168.
(7) Kelsall, G. H.; Tang, S.; Smith, A. L.; Yurdakul, S. *J. Chem. Soc., Faraday Trans.* **1996**, *92*, 3879.
(8) Manor, O.; Vakarelski, I. U.; Tang, X.; O'Shea, S. J.; Stevens, G. W.; Grieser, F.; Dagastine, R. R.; Chan, D. Y. C. *Phys. Rev. Lett.* **2008**, *101*, 24501.
(9) Manor, O.; Chan, D. Y. C. *Langmuir* **2009**, *25*, 8899.
(10) Born, M.; Wolf, E. *Principles of Optics: Electromagnetic Theory of Propagation, Interference and Diffraction of Light*, 6th ed.; Cambridge University Press: Cambridge, U.K., 1997.
(11) Bart, E. *Chem. Eng. Sci.* **1968**, *23*, 193.
(12) Brenner, H. *Chem. Eng. Sci.* **1961**, *16*, 242.
(13) Hunter, R. J., *Foundations of Colloid Science*; Oxford University Press: Oxford, U.K., 1987; Chapter 7.
(14) Yang, C.; Dabros, T.; Li, D.; Czarnecki, J.; Masliyah, J. H. *J. Colloid Interface Sci.* **2001**, *243*, 128.
(15) Munday, J. N.; Capasso, F.; Parsegian, V. A. *Nature* **2009**, *457*, 170.

JP911104B